Pharm Res (2016) 33:1881–1898
DOI 10.1007/s11095-016-1924-2

RESEARCH PAPER

Thermo-Sensitive Liposome co-Loaded of Vincristine and Doxorubicin Based on Their Similar Physicochemical Properties had Synergism on Tumor Treatment

Mingyuan Li[1] • Zhiping Li[1] • Yang Yang[1] • Zhiyuan Wang[1] • Zhenbo Yang[2] • Bingsheng Li[1] • Xiangyang Xie[3] • Jinwen Song[4] • Hui Zhang[1] • Ying Li[1] • Guangyu Gao[1] • Jingyuan Yang[5] • Xingguo Mei[1,6] • Wei Gong[1,6]

Received: 12 December 2015 / Accepted: 7 April 2016 / Published online: 13 April 2016

ABSTRACT

Purpose To develop vincristine (VCR) and doxorubicin (DOX) co-encapsulated thermo-sensitive liposomes (VD-TSL) against drug resistance, with increased tumor inhibition rate and decreased system toxicity, improving drug targeting efficiency upon mild hyperthermia (HT) in solid tumor.

Methods Based on similar physicochemical properties, VCR and DOX were co-loaded in TSL with pH gradient active loading method and characterized. The time-dependent drug release profiles at 37 and 42°C were assessed by HPLC. Then we analysed the phospholipids in filtrate after ultrafiltration and studied VD-TSL stability in mimic *in vivo* conditions and long-time storage conditions (4°C and −20°C). Cytotoxic effect was studied on PANC and sw-620 using MTT. Intracellular drug delivery was studied by confocal microscopy on HT-1080. *In vivo* imaging of TSL pharmacokinetic and biodistribution was performed on MCF-7 tumor-bearing nude mice. And therapeutic efficacy on these xenograft models were followed under HT.

Results VD-TSL had excellent particle distribution (about 90 nm), high entrapment efficiency (>95%), obvious thermo-sensitive property, and good stability. MTT proved VD-TSL had strongest cell lethality compared with other formulations. Confocal microscopy demonstrated specific accumulation of drugs in tumor cells. *In vivo* imaging proved the targeting efficiency of TSL under hyperthermia. Then therapeutic efficacy revealed synergism of VCR and DOX co-loaded in TSL, together with HT.

Conclusion VD-TSL could increase drug efficacy and decrease system toxicity, by making good use of synergism of VCR and DOX, as well as high targeting efficiency of TSL.

KEY WORDS doxorubicin · hyperthermia · solid tumor · thermo-sensitive liposome · vincristine

✉ Xingguo Mei
ddsnano@126.com

✉ Wei Gong
usnitro2004@126.com

[1] Institute of Pharmacology and Toxicology, Academy of Military Medical Sciences, Beijing 100850, People's Republic of China

[2] Pharmacy Department, No. 261 Hospital of PLA, Beijing 100094, People's Republic of China

[3] Department of Pharmacy, Wuhan General Hospital of Guangzhou Military Command, Wuhan 430070, People's Republic of China

[4] Institute of Transfusion Medicine, Academy of Military Medical Sciences, Beijing 100850, People's Republic of China

[5] School of Pharmacy, Yunnan University of Traditional Chinese Medicine, Kunming 650500, People's Republic of China

[6] Present address: No.27 Taiping Road, Haidian District, Beijing, China

ABBREVIATIONS

CVD-TSL	Thermo-sensitive liposomes containing Cou-6, vincristine and doxorubicin
Cy5-TSL	Thermo-sensitive liposomes containing Cy5
DOX	Doxorubicin
DOX-TSL	Thermo-sensitive liposomes containing doxorubicin
HT	Hyperthermia
TSL	Thermo-sensitive liposomes
VCR	Vincristine
VCR-TSL	Thermo-sensitive liposomes containing vincristine

VD-TSL Thermo-sensitive liposomes containing vincristine and doxorubicin

INTRODUCTION

Solid tumor is viewed as an organ containing multiple cell types that act in concert to promote tumor growth (1, 2). They have an aggressive histopathological appearance and have often invaded neighboring organs or disseminated throughout tissues at the time of diagnosis (3–5). Many of them have an ambiguous borderline, which leads to high relapse rate after surgical resection. Chemotherapy continues to be the first-line treatment together with radiation therapy or surgery for most cancers, but always be accompanied by undesirable systemic side effects (6, 7) and failed to drug resistance (8). Drug resistance may be defined as a deficient response to chemotherapy (intrinsic resistance) or an early response followed by progression after chemotherapy (acquired resistance) (9). The mechanisms of drug resistance include some enzyme inactivation, membrane permeability changes, blockage of drug into the target structure, the original metabolic process alterations, and so on. As a result of nonspecific drug accumulation (10), chemotherapy patients often suffer adverse side effects associated with overdose because safe dosages may not completely eradicate tumors (11).

Combination therapy seeks to increase cancer eradication efficacy without amplifying systemic toxicity while simultaneously overcoming drug resistance (12). The anthracycline anticancer drug doxorubicin (DOX) is an effective chemotherapeutic agent that is generally used for the treatment of solid tumors (13, 14). It has strong inhibitory effect on the synthesis of DNA and RNA, belonging to the cycle nonspecific anticancer drug, and its major limitation is cardiotoxicity. Doxorubicin cardiomyopathy accompanied by congestive heart failure ranges from 0.1 to 18.0% (15), and this complication is associated with a poor prognosis (14, 16). Vincaalkaloid vincristine (VCR) has also been widely used as a broad-spectrum antitumor drug since the 1960s, mainly for lymphoma and leukaemia. It has excellent therapeutic effect but a relative high neurotoxicity (17). As reported, 1 mg/kg of VCR could nearly achieve the tumor inhibitive effects of 10 mg/kg vinorelbine on tumor-bearing nude mice (18). VCR is a metaphase-specific drug that binds totubulin, causing microtubule depolymerization and apoptosis in cells during mitosis (19–21). When be administrated with DOX, VCR exerts cardio protective effects on cardiac myocyte toxicity induced by DOX, as well as chemical and hypoxicoxidative stress (22). In this way, DOX and VCR act on different targets of tumor cells, during solid tumor treatments, their combination would not only effectively surmount the drug resistance, but reduce the cardiotoxicity as well. Besides the pharmacologic characteristics above, DOX and VCR have similar physicochemical properties for synchronous co-encapsulation as Table I shows (23).

Focusing on decrease undesirable system side effects, we turned to encapsulate the two drugs above to the stimulus-sensitive drug delivery systems to increase their targeting efficiency. The purpose of this targeted drug delivery system is to concentrate drugs on targeted site, significantly decrease drug concentration in circulation and normal tissues, then reduce systemic toxicity as much as possible. TSL was first introduced by Yatvin *et al.* (24, 25), it has a triggered drug release feature around a tunable membrane phase transition temperature (Tm, 42°C) (26–28), which is obtainable by using an external microwave or a high intensity focused ultrasound (methods of mild hyperthermia) (29, 30). Owing to the enhanced permeability retention (EPR) effect, TSL (diameter – 100 nm) will accumulate into well vascularized tumors, resulting in an enhanced local accumulation first (31–35). TSL combined with HT enabled a prolonged circulation half-life and controlled drug release in the exposure site of HT (36–38), then achieve a high concentration of drug in solid tumor, touching the very boundary (39, 40), so change the drug distribution *in vivo*. In addition, tumor cell sensitivity rises as well as DNA repair activity is inhibited during HT (41). As the most advanced stimulus-sensitive drug delivery system has progressed to clinical trials in recent years. The Celsion Inc. (USA) developed DOX-TSL, named ThermoDox®(42, 43). It has apparent thermo-sensitive characteristic and effective tumor suppression, which was approved for clinical trials in 2006, and completed phaseIII trials in 2012 (44, 45). Although the results failed to meet its required endpoints for progression free survival, we understand science is never plain sailing. Just as their supplementary phaseIII trials in China, TSL is still a promising vesicle for antineoplastic agents.

In this work, a solid tumor targeting drug delivery system of VD-TSL (Thermo-sensitive liposomes containing vincristine and doxorubicin) was constructed. And the principle of drug co-encapsulation is showed in Fig. 1. The physicochemical characters, *in vitro* drug release and stability of VD-TSL within 6 months were investigated. *In vitro* and *in vivo* experiments on solid tumor were carried out to evaluate the performance of the prepared VD-TSL.

MATERIALS AND METHODS

Materials

1, 2-Dipalmitoyl-sn-glycero-3-phosphocholine (DPPC), 1-stearoyl-2-hydroxy-sn-glycero-3- phosphatidylcholine (MSPC) and 1, 2-distearoyl-sn-glycero-3-phosphoethanolamine- N-[methoxy(polyethylene glycol)-2000] (DSPE-PEG_{2000}) were purchased from Avanti (USA).

Table I Physicochemical Properties of DOX and VCR

Name	Category	Water solubility mg/ml	p Ka		log P
			Strongest Acidic	Strongest Basic	
DOX	alkaloid	1.18	9.53	8.94	1.27
VCR	alkaloid	0.03	10.85	8.66	2.82

Sulfate vincristine was obtained from Baiyunshan Company (PRC).

Preparation of Different Liposome Formulations

VCR and DOX was simultaneously loaded into liposomes, formulated with DPPC: DSPE-PEG_{2000}: *MSPC* = 75:17:8 (weight ratio) using the active loading way (46). First of all, the blank liposomes were prepared by lipid film hydration and extrusion (47). The lipids were dissolved in chloroform and the solvent was removed under vacuum in rotary evaporator forming the homogeneous lipid film, vacuum dried for 8 h. Then lipid film was hydrated in 300 mM citric acid buffer solution at 50°C for 30 min. The newly formed multilammelar lipid vesicles were shattered by homogenizer (EmulsiFlex-C3, AVESTIN, Canada) from 5000 to 15000 psi for several cycles, extruding through extruder of 200 nm polycarbonate filter at 50°C and resulted in small TSL with a uniform size (19, 48).

VCR and DOX (1:4, *w*/*w*) were loaded into the liposome using the pH gradient method at 1:20 Drug/Lipids mass ratio (49). Liposome suspension was directly added into 300 mM citric acid buffer drug solution, and then we adjusted pH of extrinsic phase to 7.5 using Na_2CO_3 solution (Fig. 1). As a result, liposomes with pH gradient between extrinsic and interior phase were developed, then incubated for about 30 min. In the end, most of drug molecular were locked in interior phase as ionotropic VCR and DOX. Then VD-TSL were filtration sterilized by 100 nm polycarbonate filter and subpackaged to aseptic pials (VCR 0.4 mg/ml, DOX 1.6 mg/ml, 1 ml/pial) (19, 50). VCR-TSL (VCR 2 mg/ml) and DOX-TSL (DOX 2 mg/ml) were prepared the same way as VD-TSL.

Quantitative Determination of Drugs

HPLC was used for the quantitative determination of VCR and DOX. The HPLC system consisted of a G1311A QuatPump, a G1315D DAD detector (Agilent, 1200 series, America). An EPC-C8 guard column and a ZORBAX SB-C8 analytical column (4.6 mm × 250 mm, pore size 5 μm) was used (51). For the detection of VCR and DOX, the mobile phase consisted of methanol: diethylamine solution (Mixture of water and diethylamine (985:15), adjusted with phosphoric acid to pH 7.5) 70:30 (*v*/*v*) introduced at a flow rate of 1 ml/min and the detection wavelength was 297 nm. (VCR: linearity: $y = 15.3\times$, $r^2 = 1$, range: 10 μg/ml - 1.2 mg/ml; DOX: linearity: $y = 13.68\times$, $r^2 = 0.999$, range: 10 μg/ml - 1.2 mg/ml; reproducibility and recovery for the method could meet the requirements.) While that for related compounds of VCR, the mobile phase is maintained at a flow rate of 1 ml/min, with an initial gradient of 62% of methanol and 38% of diethylamine solution for 12 min, then changed to increase methanol at a rate of 2% per minute, so that after 15 min it will comprise 92% of the mixture, then changed to decrease methanol at a rate of 15% per minute, so that after 2 min it will

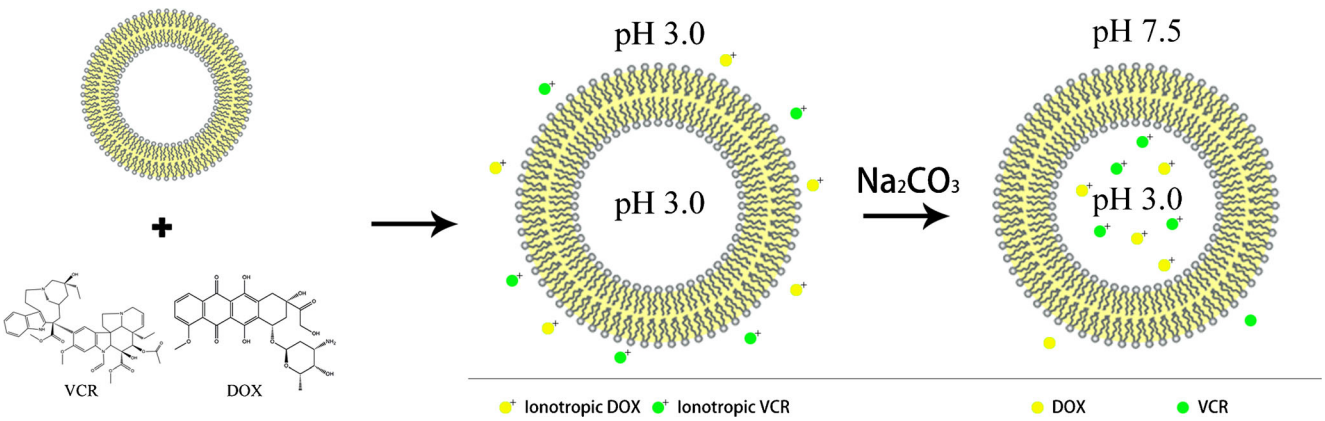

Fig. 1 The drug loading process.

again comprise 62% of the mixture. (System Suitability was good, detective limit was 3 ng/ml, and quantificative limit was 10 ng/ml.)

Entrapment Efficiency

An ultrafiltration technique was used to separate the unencapsulated VCR and DOX from liposomes. A total of 0.5 ml drug containing liposomes, which was diluted 10 times, was placed in the upper chamber of a centrifuge tube matched with an ultrafilter (Sartorius Vivaspin 500 μl, 30 k MWCO PES, Germany) and was centrifuged for 10 min at 10, 000 rpm. The ultrafiltrate in the ultrafilter containing the unencapsulated drug was determined by HPLC, as described above. The total drug in VD-TSL was determined through SDS solution (5%) disruption by HPLC. The entrapment efficiency (EE%) was calculated using the following equation:

$$EE\% = \left(W_{total\ drug} - W_{free\ drug}\right) \Big/ W_{total\ drug} * 100\%$$

Where $W_{total\ drug}$ and $W_{free\ drug}$ represent the total drug in TSL and the amount of free drug in the ultrafiltrate, respectively.

Particle Size and Zeta Potential

The particle size distribution of the liposomes was determined using photo correlation spectroscopy (Nanophox, Sympatec GmbH, Germany). Liposome suspension was diluted with distilled water to avoid multiscattering phenomena; desired temperature was 25°C; measuring mode was cross correlation. Zeta potential analysis was conducted by using a Malvern Nano-ZS90 (Malvern Instruments, UK).

TEM Cryo Imaging

The morphology of the liposome was observed by transmission electron microscopy (TEM, JEM-1010, JEOL Ltd., Tokyo, Japan). Samples for imaging were prepared by applying a 15 μl droplet of distilled water diluted liposome suspension to a Formvar-coated copper grid. Then the copper grid was air-dried for 10 min at room temperature after removing the excessive sample with filter paper. The adhered liposomes was negative stained by 3% phosphotungstic acid solution, and air-dried at room temperature (52).

In Vitro Release of Drug from Liposomes With Different Formulations

In vitro drug release from TSL with different formulation (VCR, DOX, VCR *vs* DOX) was established at 37, 39, 41 and 42°C respectively. Add TSL 1 ml into a little beaker which had 9 ml normal saline (42°C or 37°C) under stirring. The drug release was measured over time (at 1, 3, 5, 10, 30, 60 min) (52), extracting 500 μl TSL suspension and ultrafiltrating, then add additional 500 μl normal saline.

Dissolved TSL (by adding 5% sodium dodecylsulphate (10:1 *v/v*)) were considered as a positive control. The accumulated drug release (A%) was calculated using the following equations:

$$A_i(\%) = \frac{C_i \times 10 + (C_{i-1} + C_{i-2} + \ldots + C_1) \times 0.5}{C_{control} \times 10} \times 100\%$$

i-The samlping number; Ci-The concentration of Ultrafiltration filtrate; $C_{control}$-The concentration of dissolved TSL.

Phospholipid Analysis

To confirm the ultrafiltration technique used in the entrapment efficiency determination, we establish a high performance liquid chromatographic method with charged aerosol detection (HPLC-CAD, Waters e2695) for the determination of MSPC in blank TSL filtrate. The mobile phase was composed of methanol and distilled water with a flow rate of 1.0 ml/min. The detector parameters included a gas pressure of 35 psi (house nitrogen) and a range of 200 pA, and a Venusil XBP-C8 column was used (53, 54). The concentration of MSPC control solution was 20 μg/ml.

Stability Study

The *in vitro* stability of liposomes were evaluated using a Turbiscan Lab® Expert (Formulaction, L'Union, France), an innovative analytical instrument able to determine the small changes of colloidal systems (55). At predesigned time points through 6 months, 3 ml of the VD-TSL within specific cylindrical glass tubes under 4°C storage ($n = 3$) was submitted to Turbiscan Lab® Expert stability analysis. While VD-TSL under −20°C ($n = 3$) storage had to thaw first, and then be submitted to stability analysis above. And VD-TSL was also diluted by cell culture medium (90% DMEM) containing 10% FBS and analysis for 24 h. Measurements were carried out using a pulsed near infrared LED at a wavelength of 880 nm.

In Vitro Cyto Toxicity

Cytotoxicity of Blank/Heating (Blank/HT, 45°C water bath for 30 min), VCR-TSL/HT, DOX-TSL/HT, VCR *vs* DOX, VD-TSL and VD-TSL/HT was evaluated by MTT assay with sw-620 and PANC cells. sw-620 and PANC cells purchased from the Cell Resource Centre (IBMS, CAMS/PUMC) were intained in the culture medium RPMI and DMEM supplemented with 10% FBS, 100 IU/ml penicillin,

and 100 mg/ml streptomycin, respectively (56). The two kinds of cells were plated in 96 well plates at a concentration of 1×10^5 cells/well. The cells were allowed to adhere to the bottom of the wells for 24 h at 37°C with 5% CO_2 (57). After then, the plates with 20 μl of VCR-TSL (100 μg/ml), DOX-TSL (100 μg/ml) and VD-TSL (VCR: DOX =1: 4, *w/w*, 100 μg/ml in total) were placed at 42°C water bath for 30 min, as well as the Blank/HT ones. The others were added 20 μl of VCR *vs* DOX (VCR: DOX =1: 4, *w/w*, 100 μg/ml in total) and VD-TSL without HT. Then we incubated all the plates for an additional 24, 48 and 72 h, respectively. Next, 20 μl of MTT solution (5.0 mg/ml) was added to each well, and the plates were incubated for 4 h at 37°C. The media was removed and then 150 μl dimethyl sulfoxide (DMSO) was added to each well to dissolve the formazan crystals formed by the living cells. Cells without treatment were used as control (58). The absorbance at 492 nm of the solution in each well was recorded using a Microplate Reader (Model 680, BIO-RAD, USA). All samples were evaluated in sextuplicate.

Confocal Laser Scanning Microscopy (CLSM)

Following the culture of sw-620 and PANC cells for 24 h on a petri dish, DOX-TSL, DOX-TSL/HT, VCR *vs* DOX, VD-TSL, VD-TSL/HT, Cou-TSL, Cou-TSL/HT, CVD-TSL (Cou, VCR and DOX), CVD-TSL/HT were added to each dish, and incubated at 37°C for another 4 h. Then the medium was removed, and the cells were washed with cold PBS (0.1 M, pH 7.4) for 3 times, followed by fixing with 4% paraformaldehyde for 20 min. Nucleus staining was performed by Hoechst33258 for 10 min at ambient temperature. The fluorescent images of cells were analyzed via confocal laser scanning microscopy (UltraVIEWVox, PerkvnElmer, USA).

Animal Model

Female nu/nu nude mice (weighing 18–22 g) were purchased from Vital River Laboratories (Beijing, China). A xenograft tumor model was produced via subcutaneous injection of MCF-7 cells as described in our previous report (55). All procedures involving animal housing and treatment were approved by the Animal Care and Use Ethics Committee of the Academy of Military Medical Sciences. Upon reaching tumor size of about 5 mm in diameter after 10 days growth, we began to prepare for the following experiments.

In Vivo Imaging

The MCF-7 xenografted nude mice were received tail i.v. with 200 ul of 5% glucose (control), free Cy5 or Cy5-TSL at 1.2 mg/kg. Half of Cy5-TSL mice had HT treatment after administration. HT treatment was as follow: After injection, the mice were fixed on heat insulation board by rubber band. The board had temperature-controlled holes, and tumor was placed above the holes. Temperature of holes was controlled at about 42°C by copper stick which had one terminal into hot water bath (45°C), and gave HT to tumor location for 30 min. Subsequently, *in vivo* fluorescence imaging was performed with a IVIS® Lumina II *in vivo* imaging system (IVIS® Lumina II *In Vivo* Imaging System, Caliper life sciences, USA) at the indicated times (15 min, 30 min, 1 h, 6 h and 24 h after injection). After *in vivo* imaging, the mice were sacrificed by cervical dislocation, and the tumor and major organs, including heart, liver, spleen, lung, kidney, were excised and imaged.

In Vivo Antitumor Efficacy

40 nude mice bearing similar sized tumor were selected from 70 ones, then randomly divided into five groups. Control group (CG) received tail i.v. of physiologic saline; Injection group (IG) was given tail i.v. of VCR *vs* DOX solution (VCR 0.2 mg/kg, DOX 0.8 mg/kg); VCR-TSL/HT group (VG) was administrated tail i.v. of VCR-TSL(1.0 mg/kg) then had HT treatment; DOX-TSL/HT group (DG) was DOX-TSL(1.0 mg/kg) suspension with HT treatment and VD-TSL/HT group (VDG) was VD-TSL (VCR 0.2 mg/kg, DOX 0.8 mg/kg) (55).

Mice were subjected to treatment every 72 h, three treatments were given in all. During treatment, major and minor diameter of tumor was determined every day. Calculate volume according to formula1: $V = 1/2 * L * S^2$, where L was major and S was minor diameter. Three days after the last treatment, mice were executed. Their tumors were deprived and weighed. Based on the data, growth curves of tumor were drawn and tumor inhibition rate (IR) was calculated as formula 2: $IR = (1 - m/mc) * 100\%$. The mc was the average weight of tumor in control group, m was average weight of tumor in other experimental groups (56).

Statistical Analysis

All data are shown as means standard deviation (SD) unless particularly outlined. Student's *t* test or one-way analyses of variance (ANOVA) were performed in statistical evaluation. A P-value less than 0.05 was considered to be significant, and a P-value less than 0.01 was considered as highly significant.

RESULTS

Preparation and Characterization of Liposomal Formulations

A drug delivery system based on the temperature-triggered VCR and DOX release of TSL was proposed for the targeted

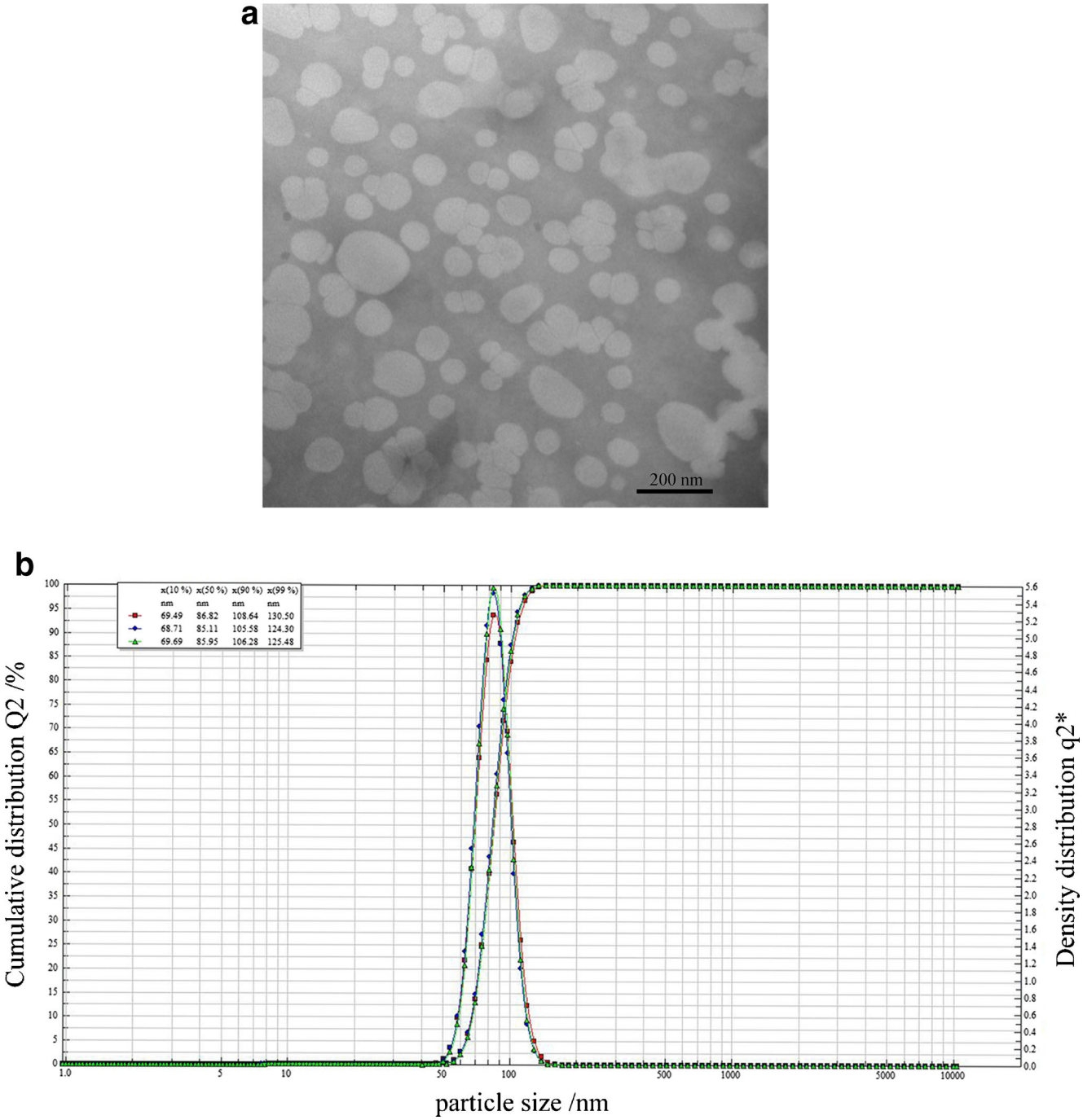

Fig. 2 TEM imaging of TSL (**a**); Particle size distribution of TSL (**b**).

Table II Characterization of Blank Liposome and Drug Loaded TSLs ($n = 3$)

Batch	Size (X_{50}, nm)	pH	Zeta potential (mV)	Drug content (mg/ml)	Entrapment efficiency (%)
Blank liposome	85.23 ± 2.03	3.02 ± 0.12	2.13 ± 0.21	———	———
VCR-TSl	90.03 ± 0.28	7.31 ± 0.22	0.33 ± 0.10	2.05 ± 0.05	98.21 ± 1.55
DOX-TSL	88.45 ± 1.41	7.26 ± 0.14	−1.27 ± 0.06	2.02 ± 0.11	97.39 ± 0.84
VD-TSL	90.12 ± 0.86	7.36 ± 0.06	−0.69 ± 0.39	2.01 ± 0.10	97.84 ± 1.23

delivery of drugs to tumor cells. Transmembrane gradient-loading methods have been used to actively encapsulate amphipathic weak bases into liposomes with high entrapment efficiency. These include simple pH gradients, ammonium gradients, $MnSO_4$ gradients, and so on. Both VCR and DOX are amphipathic weak bases with similar pKa (Table I), and we loaded them into liposomes by pH-gradient. Instead of eluting dextran gel (G50) column, we directly dropped Na_2CO_3 solution to exterior phase of TSL generating gradient. This method was simple, quick and obtained high entrapment efficiency.

Three TSLs, including DOX-TSL, VCR-TSL and VD-TSL, were fabricated via the film evaporation/ultrasonication method. The morphology (Fig. 2) of the fabricated liposomes had a regular circular shape. The mean diameter, pH, assay and encapsulation efficiency of the liposomes were exhibited in Table II. The results showed all the liposomes had a mean particle size of about 90 nm, and an encapsulation efficiency of about 98%. The zeta potential of VD-TSL was near zero because DPPC, MSPC and DSPE-PEG_{2000} were all electric neutrality.

Temperature Triggered Release of Different Formulations

Whether different drug had an influence on drug release under heat stimulus is crucial for the success of the targeting liposomal system. The release of DOX and VCR from VCR-TSL, DOX-TSL, VD-TSL at different temperatures (37, 39, 41 and 42°C) was depicted in Fig. 3. The data revealed the release of both DOX and VCR from various liposomes exhibited a temperature-dependent characteristic, and was considerably low at 37°C (released less than 10% of total amounts after heating for 30 min). However, the release amount of both payloads approached about 85% within the first 5 min of heating at 42°C. At the end of HT process there was still 8–10% of the encapsulated DOX or VCR remained in carriers. The statistical differences of the 3 TSL formulations were not significant.

Phospholipid Analysis

We analyzed the filtrate and MSPC solution. As shown in Fig. 4a, the peak b, c and d were the special peaks for MSPC, the peak a was methol. While in Fig. 4b, peak e was water, and the large peak after it was sugar and inorganic salts (59). We recognized that none of specific peaks for MSPC could be found in Fig. 4b, indicating that there was no phospholipid in filtrate after ultrafiltration of blank TSL. The figure suggested the rationality of ultrafiltration in TSL entrapment efficiency determination.

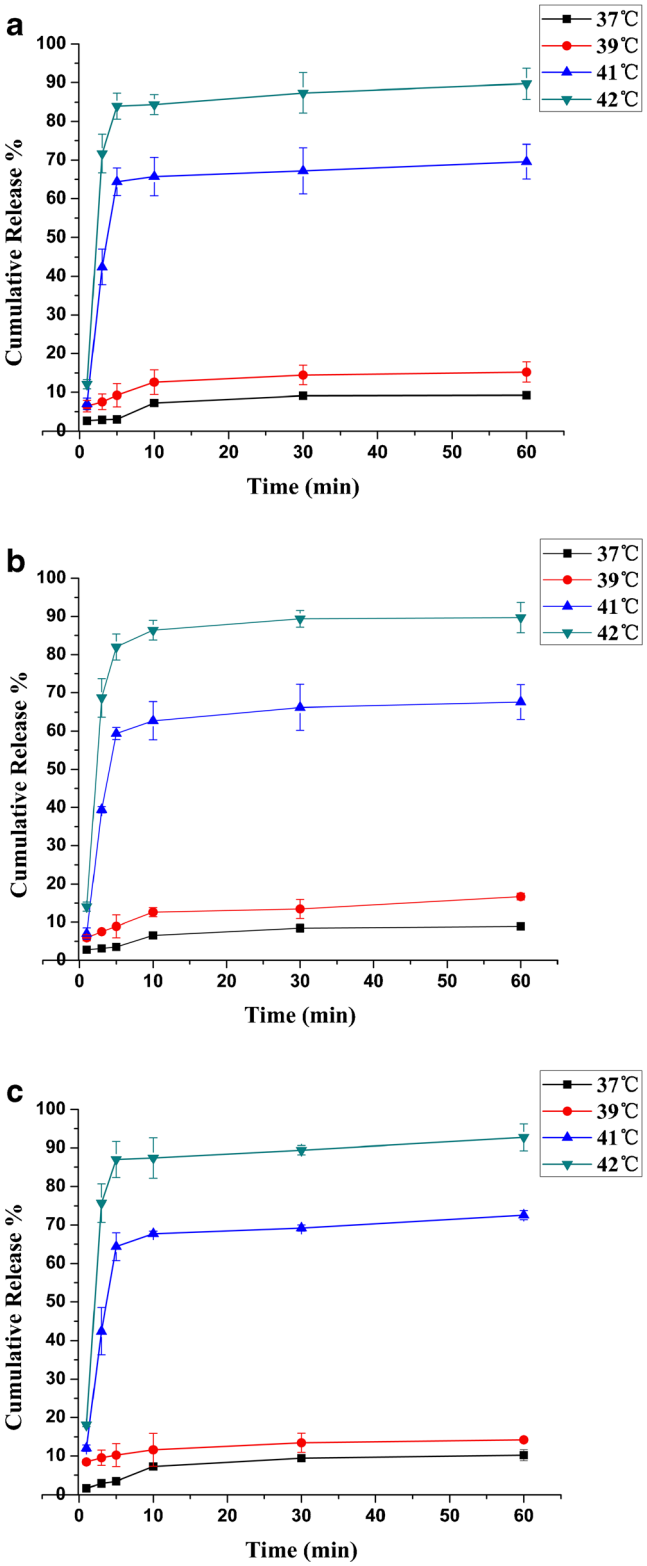

Fig. 3 Temperature-triggered release behaviors of VCR (**a**), DOX (**b**) and VCR *vs* DOX (**c**) from the fabricated TSLs at 37, 39, 41, and 42°C, respectively ($n = 3$).

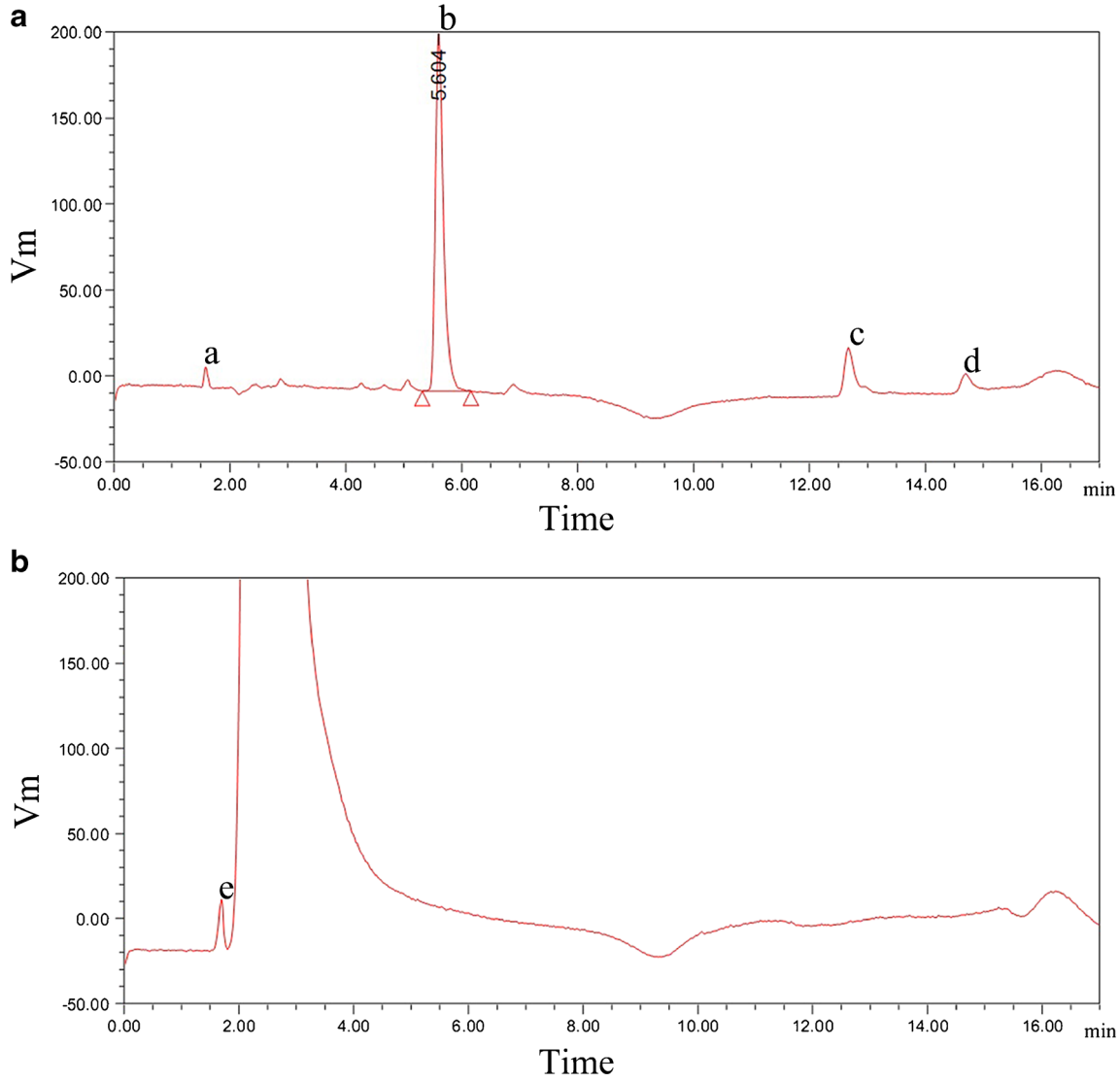

Fig. 4 CAD evaluation of 20 μg/ml MSPC (**a**); CAD evaluation of vincristine TSL filtrate after ultrafiltrate (**b**).

Stability Study

The stability of VD-TSL is an important aspect to be taken into account when further used *in vivo* as product. The occurrence of aggregation, deposition and hydrolysis phenomena of VD-TSL under storage can lead to significantly worsening of the biopharmaceutical features of the vesicles. So the stability of VD-TSL diluted by cell culture medium for 24 h (37°C) and stored under 4°C, −20°C within 6 months was evaluated using the Turbiscan Lab® Expert. Variations greater than 10% either as a positive or negative value in the graphical scale of backscattering are the representative of an instable formulation (55). According to this judgement, the transmission or back-scattering profiles obtained (Fig. 5) indicating there was no apparent aggregation or sedimentation occurred of VD-TSL under each situation.

The particle size variations in Tables III and IV indicated that there had been some hydrolysis and oxidation of VCR under 4°C, since the liquid suspension of VCR is not a stable long-term storage state. But the morphology of TSL stored under 4°C was still stable. Each time we evaluated VD-TSL stored under −20°C, they were melt first and frozen again after evaluation. Their size increased a little within proper range because of the generation of ice crystal, and the evaluative operation also proved that VD-TSL had excellent frozen-melt stability. Besides size variations, we also take other

Fig. 5 Transmission and backscattering profiles of VD-TSL by using Turbiscan Lab® Expert. The image (**a** and **b**) represent the analysis of different storage conditions within 6 months: 4°C and −20°C, respectively. And the stability of VD-TSL diluted by cell culture medium for 24 h at 37°C (C). Data are reported as a function of time and sample height (from 28 to 48 mm).

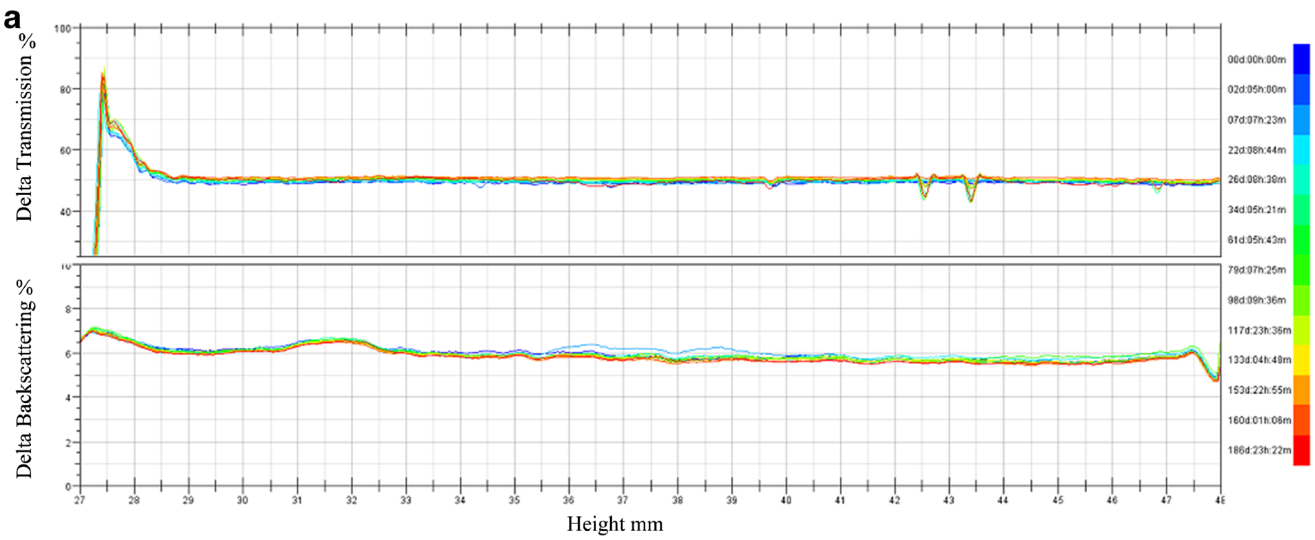
a
Delta Transmission %
Delta Backscattering %
Height mm
00d:00h:00m
02d:05h:00m
07d:07h:23m
22d:08h:44m
26d:08h:38m
34d:05h:21m
61d:05h:43m
79d:07h:25m
98d:09h:36m
117d:23h:36m
133d:04h:48m
153d:22h:55m
160d:01h:08m
186d:23h:22m

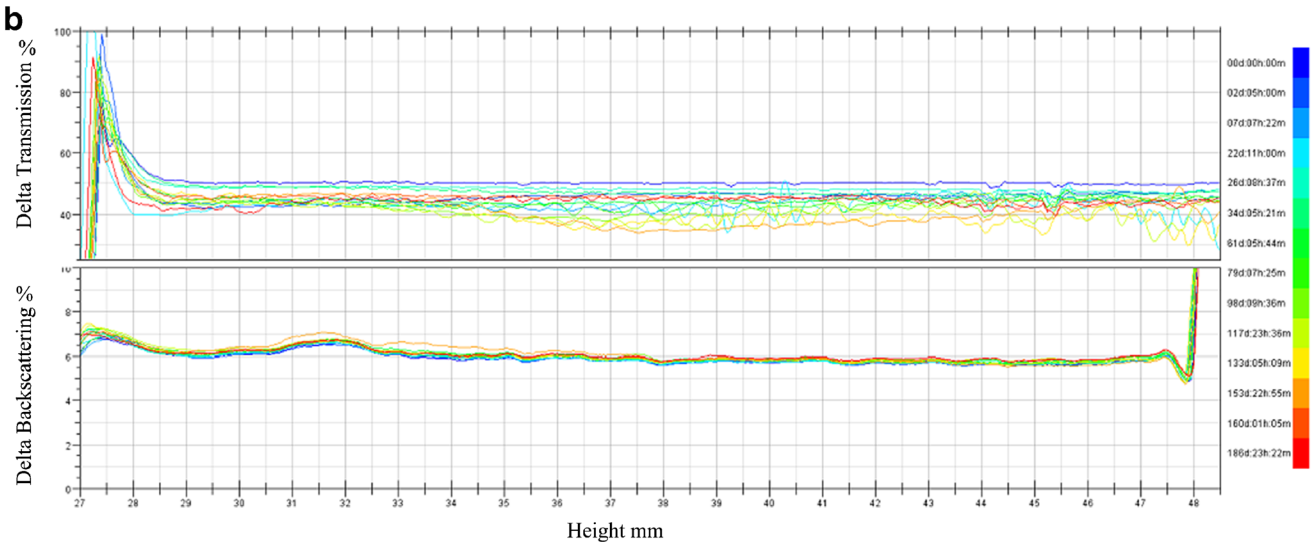
b
Delta Transmission %
Delta Backscattering %
Height mm
00d:00h:00m
02d:05h:00m
07d:07h:22m
22d:11h:00m
26d:08h:37m
34d:05h:21m
61d:05h:44m
79d:07h:25m
98d:09h:36m
117d:23h:36m
133d:05h:09m
153d:22h:55m
160d:01h:05m
186d:23h:22m

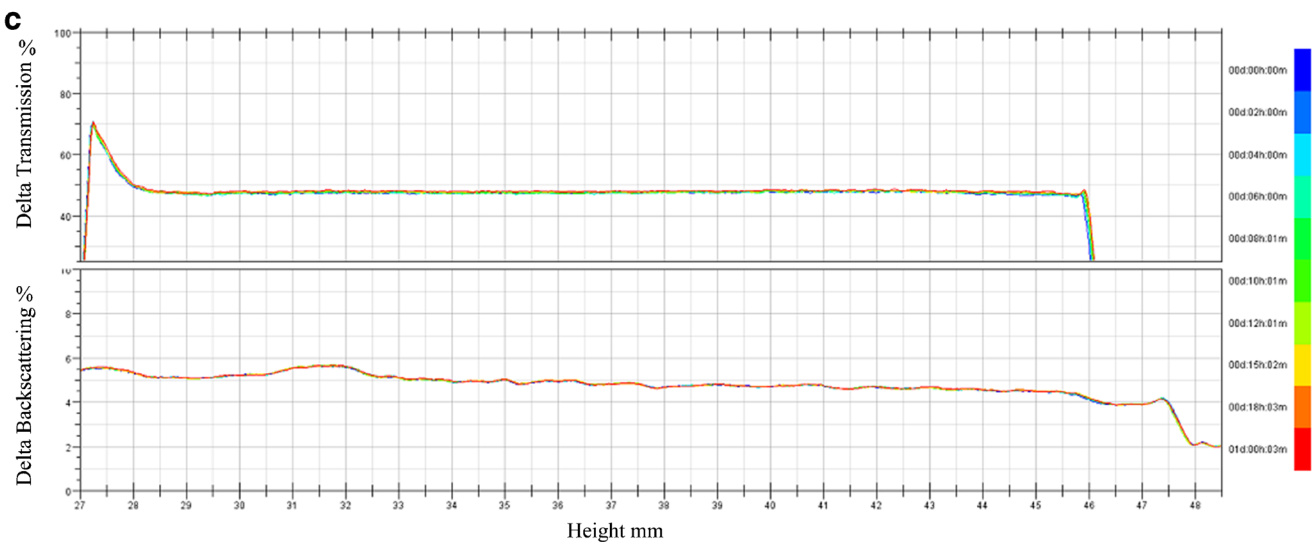
c
Delta Transmission %
Delta Backscattering %
Height mm
00d:00h:00m
00d:02h:00m
00d:04h:00m
00d:06h:00m
00d:08h:01m
00d:10h:01m
00d:12h:01m
00d:15h:02m
00d:18h:03m
01d:00h:03m

Table III The Physico-chemical Changes of VD-TSL Within 6 Months Under 4°C ($n = 3$)

Months	Size (X_{50}, nm)	VCR Related compounds (%)		Entrapment efficiency (%)
		Individual Related compounds	Total Related compounds	
1	82.10 ± 3.21	3.07 ± 0.02	5.07 ± 0.02	98.70 ± 0.01
2	79.16 ± 2.50	4.00 ± 0.01	6.40 ± 0.02	98.43 ± 0.02
3	79.42 ± 0.84	4.74 ± 0.02	7.07 ± 0.03	97.89 ± 0.01
4	79.28 ± 1.56	7.47 ± 0.01	9.09 ± 0.01	96.34 ± 0.02
5	79.10 ± 1.12	8.19 ± 0.01	10.15 ± 0.05	96.85 ± 0.03
6	75.26 ± 2.43	9.39 ± 0.04	10.63 ± 0.03	96.84 ± 0.02

factors into consideration in VD-TSL study as depicted in Tables II and III. According to the United States Pharmacopoeia, the individual related compounds of VCR shall not be greater than 2% and the total related compounds shall not be greater than 5%. After comparison, we draw a conclusion for VD-TSL: −20°C for long-term storage, and short-term deposit under 4°C.

HEAT MEDIATED CYTOTOXICITY *IN VITRO*

In Vitro Cytotoxicity of the Liposomes

The *in vitro* cytotoxicity of Blank/HT, VCR-TSL/HT, DOX-TSL/HT, VCR *vs* DOX, VD-TSL and VD-TSL/HT were tested in PANC and sw-620 cells using a MTT assay. As shown in Fig. 6, the cell viability decreased as prolonging the cell culture time with various TSLs. The results depicted VD-TSL showed stronger anti-proliferative activity than VCR *vs* DOX in both PANC and sw-620cell lines. The TSL with HT promoted anti-proliferative activities in solid tumor cell lines. VD-TSL/HT and VCR-TSL/HT showed the strongest cytotoxicity on PANC cells, followed by VD-TSL, VCR *vs* DOX, DOX-TSL/HT and Blank/HT, respectively. The data also verified that TSLs had higher drug penetration than free drugs through membrane fusion. On the other hand, HT could improve cell permeability, VCR-TSL/HT, DOX-TSL/HT and VD-TSL/HT groups also boost cytotoxicity of the liposomes to sw-620 cells. HT made damages to cells, but the cell viability hadn't decreased as prolonging the cell culture time. It could raise the membrane fluidity of cells, and opening doors for drugs ingression, that's why VD-TSL/HT had apparently stronger anti-proliferative activities than VCR *vs* DOX. The results confirmed that sw-620 cells were more sensitive than PANC cells to VCR and DOX (Fig. 6), and heat-stimulus promoted anti-proliferative activities of drugs to solid tumor cells. Comparing DOX-TSL/HT and VCR-TSL/HT with VD-TSL/HT, it was noted that DOX and VCR had apparent synergism as many clinical trials reported (60–64).

Confocal Microscopy Analysis

The cytotoxicity and cell penetrating efficiency of TSL was further evaluated by confocal laser scanning microscopy. In order to clarify the internalization of the liposomes, the cell nuclei were stained with Hoechst33258 (blue), the DOX-TSL and VD-TSL had red fluorescence (DOX), Cou-TSL had green fluorescence (Cou-6). Then the CVD-TSL had red fluorescence and green fluorescence. As shown in Fig. 7a, the red

Table IV The Physico-chemical Changes of VD-TSL Within 6 Months Under −20°C ($n = 3$)

Months	Size (X_{50}, nm)	VCR Related compounds (%)		Entrapment efficiency (%)
		Individual Related compounds	Total Related compounds	
1	85.10 ± 3.22	0.63 ± 0.01	1.22 ± 0.01	98.88 ± 0.01
2	85.96 ± 1.89	0.91 ± 0.01	1.50 ± 0.02	98.81 ± 0.02
3	91.22 ± 2.95	1.36 ± 0.02	2.15 ± 0.01	98.75 ± 0.03
4	93.46 ± 0.78	1.70 ± 0.01	2.43 ± 0.00	98.53 ± 0.02
5	93.55 ± 4.01	1.86 ± 0.00	2.55 ± 0.01	98.00 ± 0.01
6	92.11 ± 1.56	1.87 ± 0.01	3.16 ± 0.02	98.88 ± 0.01

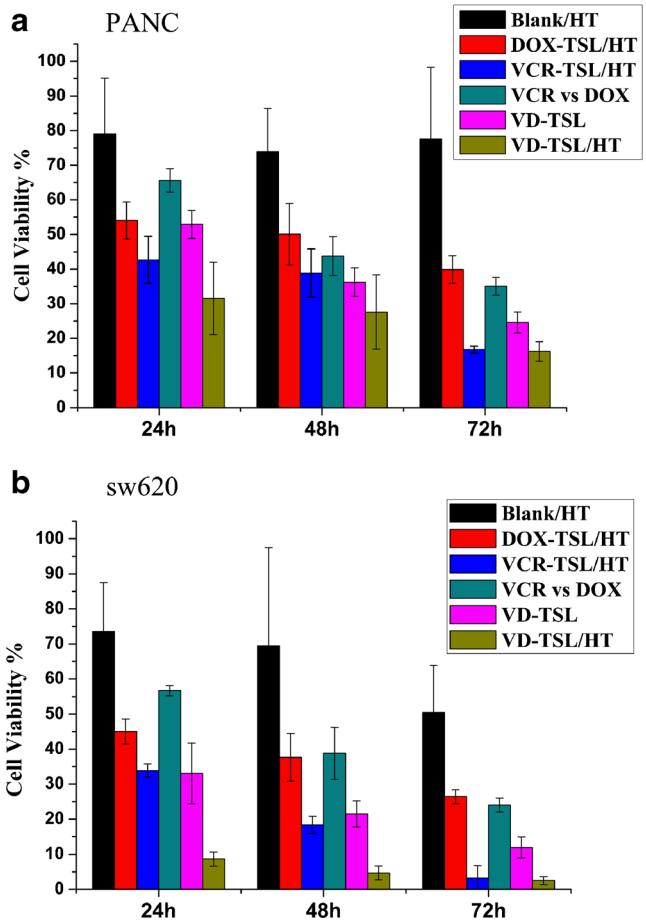

Fig. 6 ntiproliferative activity of Blank/HT, DOX-TSL/HT, VCR-TSL/HT, VCR *vs* DOX solution, VD-TSL and VD-TSL/HT. (**a**) Cell viability of PANC cells after incubating with various formulations with different times. The data are presented as the mean ± SD ($n = 6$). Blank/HT $P < 0.01$ *versus* VD-TSL/HT; VD-TSL/HT $P < 0.05$ *versus* VD-TSL; VD-TSL/HT $P < 0.05$ *versus* VCR *vs* DOX solution; VD-TSL/HT $P < 0.05$ *versus* DOX-TSL/HT; VD-TSL/HT $P > 0.05$ *versus* VCR-TSL/HT. (**b**) Cell viability of sw-620 cells after incubating with various formulations with different times. Blank/HT $P < 0.01$($n = 6$) *versus* VD-TSL/HT; VD-TSL/HT $P < 0.05$ *versus* VD-TSL; VD-TSL/HT $P < 0.05$ *versus* VCR *vs* DOX solution; VD-TSL/HT $P < 0.05$ *versus* DOX-TSL/HT; VD-TSL/HT $P < 0.05$ *versus* VCR-TSL/HT.

fluorescence (in the web version) can be found distributing mainly in the nuclei of the HT-1080 cells treated with formulations containing DOX. DOX-TSL and VD-TSL had stronger red fluorescence intensity than DOX *vs* VCR, indicating that phospholipid membrane was better for drug entrance to cells through fusion effect. When given hyperthermia stimulus, the membrane permeability of cells would be apparent improved, as Fig. 7b. Cou-TSL/HT had stronger green fluorescence intensity in cytoplasm of the HT-1080 cells than Cou-TSL. Fig. 7c indicates the accumulation of CVD-TSL in the HT-1080 cells with and without hyperthermia, respectively. According to the images, CVD-TSL with hyperthermia exhibited the most intense intracellular fluorescence in HT-1080 cells as expected. CVD-TSL/HT represented the behavior of VD-TSL/HT in cells. With Cou-6 distributed in TSL membrane, CVD-TSL/HT had a more clear presentation that TSL could entered cells totally through membrane fusion.

IN VIVO ANTI-TUMOR EFFICIENCY OF THE TARGETED LIPOSOMES

In Vivo Distribution of TSL

Having demonstrated the efficiency in solid tumor cells *in vitro*, we next explored the activity of free drugs and TSL in MCF-7 tumor-bearing Nu/Nu nude mice models. Cy5 integrates with high stability into liposome and remains attached even when in contact with other membranes. To determine the real-time biodistribution of TSL, Cy5-labeled liposomes were administrated to MCF-7 xenograft models through tail i.v., then the time-dependent clearance and *in vivo* targeting efficacy of formulations were observed using non-invasive imaging in live animals (Fig. 8a). A strong signal was observed in the whole body within 15 min post the injection of Cy5-labeled formulations without obvious targeting effect, and gradually decreased as the time elapsed, indicating the rapid circulation of formulations in the blood stream. By monitoring real-time fluorescence intensity in the whole body, the targeting characteristics of the formulations were easily determined 30 min later. Cy5 solution showed nonspecific distribution of flurescence all over the body, and the fluorescence intensity decreased rapidly post injection. However, the fluorescence was still detectable at 12 h after administration of Cy5-TSL and Cy5-TSL/HT, indicating a prolonged circulation of the nanocarriers. Cy5-TSL/HT showed the strongest fluorescence signal in the tumor among the formulations, suggesting that Cy5-TSL/HT preferentially released Cy5 around tumor tissues, and made Cy5 accumulated in the tumor.

For a more accurate measurement, major internal organs (heart, liver, spleen, lung, kidney and tumor) were taken at 12 h post injection and analyzed directly on the fluorescent imager (Fig. 8b). The fluorescence level of Cy5-TSL and Cy5-TSL/HT in liver was observed to be higher than that of the Cy5 solution. The increase in liver accumulation of Cy5-TSL and Cy5-TSL/HT may be due to the reticuloendothelial system (RES) filtration (65). However, the fluorescence intensity of Cy5-TSL/HT in the tumor was significantly higher than other groups, which was resulted from the synergistic reaction of hyperthermia and EPR effect (66) of tumors.

In Vivo Therapeutic Efficacy

The antitumor efficacy against the MCF-7 xenograft was evaluated by comparing 1) control group, 2) VCR *vs* DOX solution, 3) VCR-TSL/HT, 4) DOX-TSL/HT, 5)VD-TSL/HT.

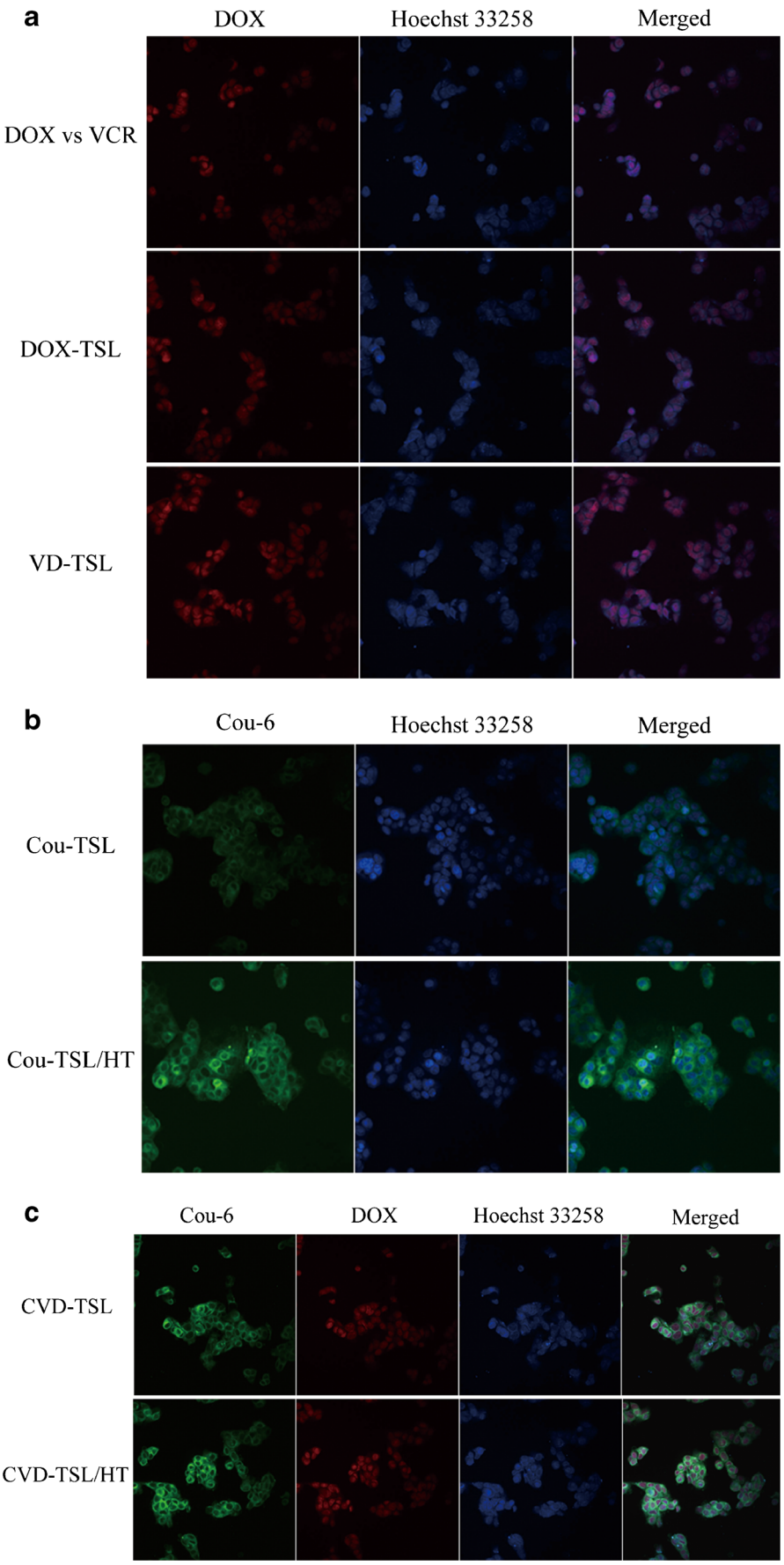
a
DOX
Hoechst 33258
Merged
DOX vs VCR
DOX-TSL
VD-TSL
b
Cou-6
Hoechst 33258
Merged
Cou-TSL
Cou-TSL/HT
c
Cou-6
DOX
Hoechst 33258
Merged
CVD-TSL
CVD-TSL/HT

◀ **Fig. 7** Cellular localization of each formulation monitored by confocal microscopy after incubating with HT-1080 cells for 4 h. (**a**) DOX *vs* VCR solution, DOX-TSL, VD-TSL, all of them without HT; (**b**) Cou-TSL and Cou-TSL/HT; (**c**) CVD-TSL and CVD-TSL/HT.

Although all treatment groups (groups 2–5) showed initial tumor regression, only the liposome co-encapsulated formulation showed significant tumor regression as well as acceptable body weight decrease. As shown in Fig. 9a, the tumor volume of mice receiving physiological saline as control (C) rapidly increased in 22 days. Under HT, the tumor inhibitive effect was in the order of VCR-TSL/HT (1.0 mg/kg) > VD-TSL/HT (1.0 mg/kg) > DOX-TSL/HT (1.0 mg/kg) > VCR *vs* DOX solution (Injection, 1.0 mg/kg).

The body weight variations over the treatment period were also monitored to estimate the toxic side-effects of each group. As shown in Fig. 9b, there was apparent reduction in body weight of the nude mice groups: VCR-TSL/HT > DOX-TSL/HT and VCR *vs* DOX solution > VD-TSL/HT. Compared with VCR *vs* DOX solution, VD-TSL/HT had stronger tumor inhibitive effect ($P < 0.05$) and less body weight reduction ($P < 0.05$), indicating TSL/HT is safer and more effective than solution. As shown in Fig. 9c, the strongest inhibitory effect was observed at the end of the study (day 22) in VCR-TSL/HT group, which exhibited an inhibitory value of $78.2 \pm 4.7\%$. Although VD-TSL/HT had an inhibitory value of $76.8 \pm 5.3\%$, this group had no significant difference with VCR-TSL/HT ($P > 0.05$). And the tumors were shown in Fig. 9d with apparent size differences.

DISCUSSIONS

Based on ThermoDox, the blank TSL contained DPPC, MSPC and DSPE-PEG_{2000}. DPPC is the fundamental composition, and it has a phase transition temperature (Tm) at 42°C. MSPC is the minimum ingredient, as a lysophosphatide, it acts as catalyst to broke lipid bilayer. The addition of DSPE-PEG_{2000} could help TSL escape from phagocytosis of RES. By addition of DSPE-PEG_{2000}, we

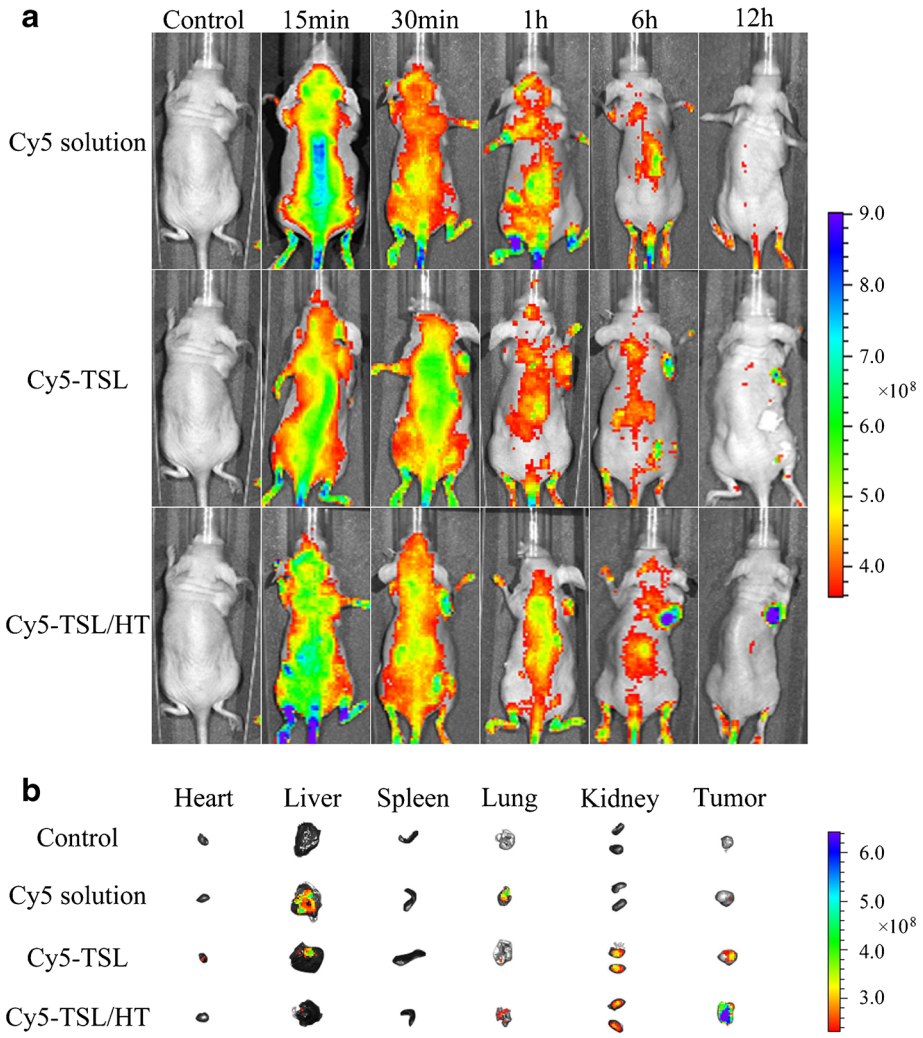

Fig. 8 Biodistribution of Cy5 during different formulations in mice bearing MCF-7 tumor xenografts. Whole body imaging at different time points after systemic administration (**a**). Fluorescence detections of isolated main tissues and organs from mice at the end point of observation (**b**).

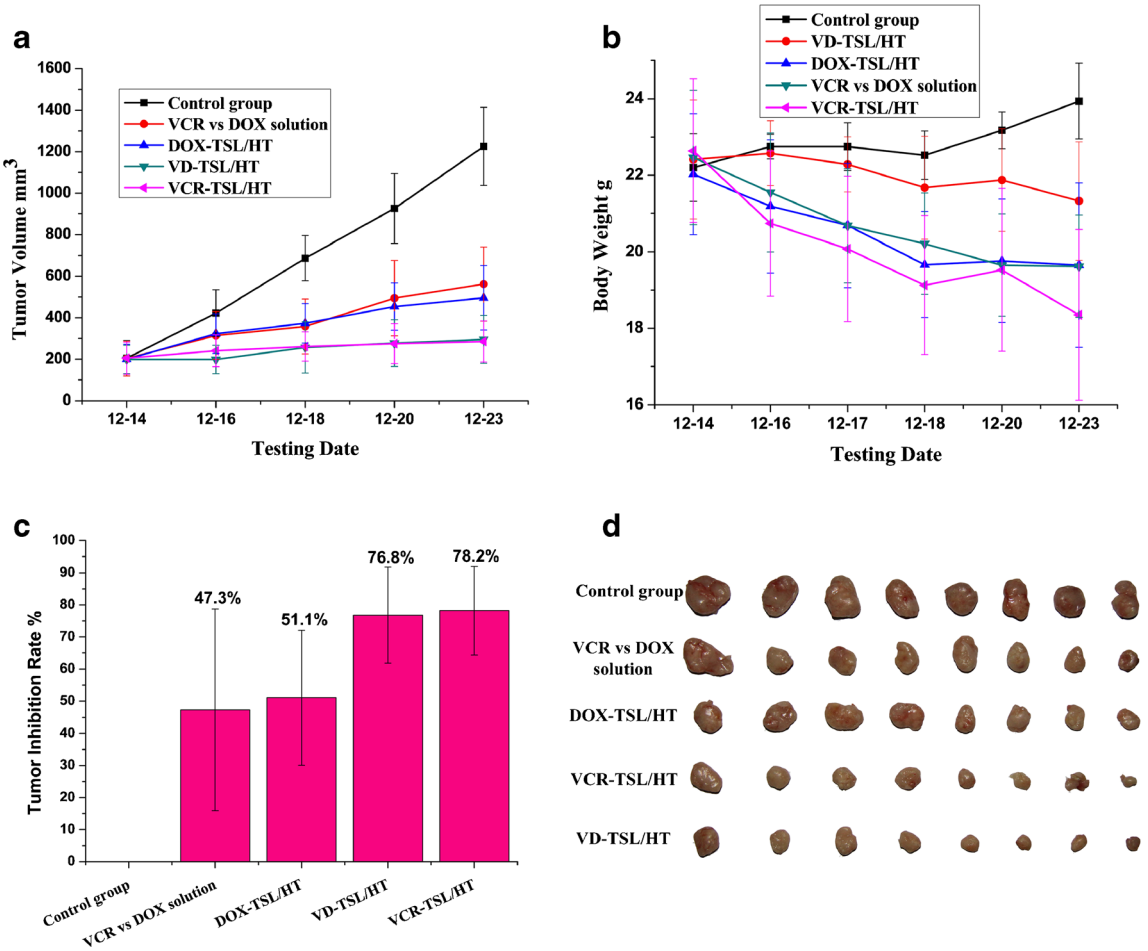

Fig. 9 Anticancer efficacy in the MCF-7 xenografts in female nude mice after the treatment with varying formulations (**a**); Body weight changes of the tumor-bearing nude mice after the treatment with varying formulations (**b**); Tumor inhibition rate of varying formulations in tumor-bearing nude mice (**c**); MCF-7 tumor inhibition experiments of VTSL on tumor-bearing nude mice (**d**). Data are presented as mean ± SD ($n = 8$).

extended the *in vivo* circulation time of liposomes; and through ratio screening, we obtained the desired Tm (67–69). Then the TSL could make use of the EPR effect to targeting accumulate in tumor tissues before triggering drug release with application of HT (70, 71). And the action mechanism of VD-TSL *in vivo* was shown in Fig. 10.

Besides the synergistic effects of VCR and DOX proved by above experiments, their similar physicochemical properties make it possible to achieve convenient co-encapsulation and synchronous quantitative determination. Both VCR and DOX are alkaloid, they have proximal pKa and high membrane permeability (The cell membrane permeability of DOX is 7.4×10^{-5} cm/s, while cell membrane permeability of VCR is even stronger) (23, 72). Because of these, we used pH gradient method to encapsulate VCR and DOX, the interior phase pH was 3.0 and the extrinsic phase pH was 7.5. Drug in extrinsic phase are molecular, then they got through lipid bilayer into interior phase becoming ions and could not get out anymore (Fig. 1).

During the assay determination of VCR and DOX in VD-TSL, first we use Triton X-100 to break TSL bilayer, but the HPLC results showed that Triton X-100 could generate some related substance with VCR, influencing the final results. Then, we used SDS solution (5%) as rupture agent of TSL instead of Triton X-100, and this hasn't been reported before. The rationale of this replace is that surfactant could break lipid bilayer, more other surfactants could also act as rupture agent for any requirements, not only SDS solution (5%).

As Fig. 3 showed, VCR and DOX had no influence with thermo-sensitive property of TSL. Tm of TSL relates to the composition of lipid bilayer, not interior phase loaded water-soluble drugs. TSL has a broad-spectrum for drug loading.

There were 3 kinds of phospholipids in VD-TSL membrane, we chose MSPC for analysis because its specific peaks have a clear separation with sugar or inorganic salts. From VD-TSL preparation depicted above, the concentration of MSPC in diluted liposomes before ultrafiltration was about 320 μg/ml, and we used 20 μg/ml of MSPC as standard

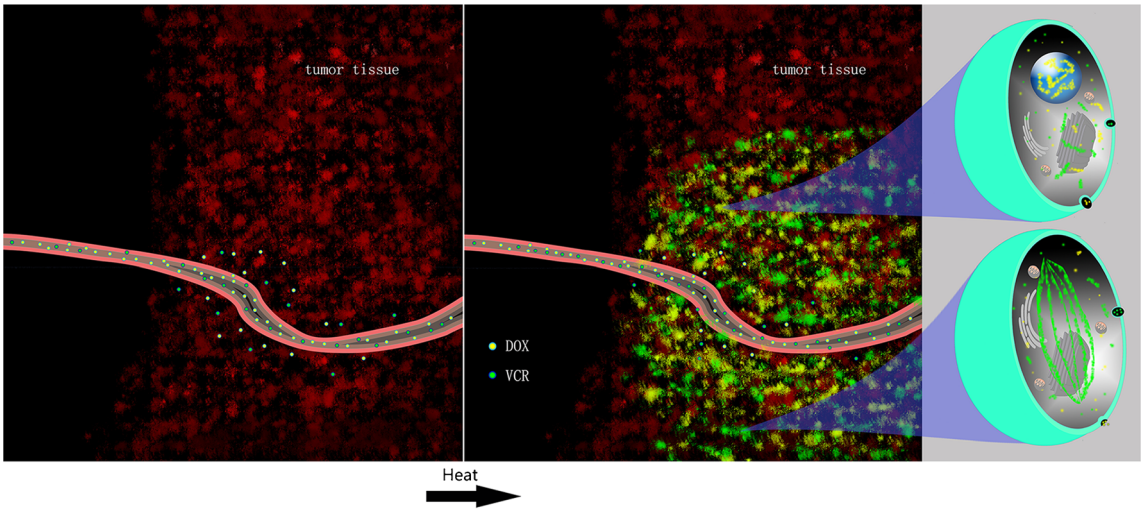

Fig. 10 After VD-TSL got into human body, which was loaded with DOX and VCR simultaneously, it would systemic distribute along with blood circulation. The VD-TSL flowing through tumor tissue could enter interstitial space through cracks in the vessel wall. When tumor tissue was given local hyperthermia, drug in VD-TSL released rapidly and accumulated in tumor. DOX mainly acts on DNA, while the main function of VCR is on tubulin, they two have synergistic effect.

solution when evaluating MSPC in filtrate. The calculation was as blow:

In VD-TSL constructed above, drug was 2 mg/ml, according to the drug/lipids ratio (1:20), phospholipids concentration was 40 mg/ml. For MSPC took 8% weight proportion of phospholipids, its concentration was 3.2 mg/ml. Diluted 10 times before ultrafiltration, then the final concentration of MSPC was 320 μg/ml.

A salient feature of the Turbiscan Lab® Expert detection is that it can detect the early small changes in transmission profiles before the appearance of a macroscopic scale physical modification of colloidal emulsions, thus shorten the lapse of time necessary for the identification of instability phenomena (73, 74). After comparison of −20 and 4°C storage (Fig. 5, Tables III and IV), we can see the related substances of VCR of VD-TSL under 4°C storage has exceeded the United States Pharmacopoeia regulations (51), while −20°C storage ones were still qualified within 6 months. For VD-TSL, −20°C is fit for long-term storage, and short-term deposit under 4°C.

The occurrence of aggregation phenomena of TSLs *in vivo* could lead to significant worsening of the biopharmaceutical features of the vesicles. So cell culture medium containing 10% FBS was used to mimic the *in vivo* situation, and the stability of VD-TSL in this medium was also evaluated by the Turbiscan Lab® Expert. The results indicating that the VD-TSL could maintain morphous stable and be applicated *in vivo*.

After confirming that VD-TSL could work properly with HT and has good stability, we assessed its ability to deliver drugs into tumor cells. *In vitro* cell experiments were performed on PANC, sw-620 and HT-1080. For the temperature triggered release property of VD-TSL, it has broad-spectrum of solid tumors. The cytotoxicity results (Fig. 6) demonstrated: (1) VCR and DOX had synergism; (2) TSL had stronger cell toxicity than solutions; (3) HT could improve the lethality of drugs and TSLs to tumor cells; (4) VD-TSL/HT had the most serious toxicity to tumor cells. CLSM experiments (Fig. 7) indicated: (1) From the comparison from DOX *vs* VCR to DOX-TSL and VD-TSL, we can see the later two had stronger fluorescence intensity, because it was easier for TSL to delivery drugs into cells than normal drug solutions; (2) The different fluorescence intensity of Cou-TSL and Cou-TSL/HT proved HT could trigger the drug release from TSL permeating into cells; (3) For CVD-TSL and CVD-TSL/HT, the latter one achieved stronger fluorescence intensity, there was a obvious red fluorescence (DOX) signal in nuclei, blocking DNA replication. The TSL membrane fragments containing Cou-6 aggregated in cytoplasm, or fused with cell membrane. VCR had no fluorescence, and couldn't be represented in Fig. 7c. For VCR affects microtubule protein, it must have stayed in cytoplasm. In this way, CVD-TSL killed tumor cells with nuclei ways and cytoplasm methods (75, 76).

The xenograft results revealed that VD-TSL/HT group had a much higher tumor inhibitory rate than VCR *vs* DOX solution (Fig. 9a). Based on high inhibitory rate, VD-TSL/HT group had significant lower toxicity to mice, when compared with VCR-TSL/HT or DOX-TSL/HT (Fig. 9b). The reasons could be explained by the following aspects: First of all, the combination of VCR and DOX had a significant synergistic effect, and the addition of VCR could reduce the cardiotoxicity of DOX, which is much better than that of single use; Second, the long-circulatory effect and suitable particle size of TSLs contributed to enough drug concentration during HT treatment by escaping from the RES rapid elimination; Third, as reported by Benjamin *et al.* (77), mild

HT augmented the accumulation of TSLs at tumor sites, and the effect was doubling the accumulation for every increase in degree from 39 to 42°C (Fig. 8). Because of the enhanced specific targeting property of the constructed drug delivery system, VD-TSL could decrease whole body toxicity of VCR and DOX to a great extent, as *in vivo* experiments finally indicated (Fig. 9b).

With additional research and preclinical studies of TSLs underway, experts explore the use of high frequency ultrasound (HiFu) as a heating modality for human beings. This kind of mild HT has been routinely used in the clinic and is known to have strongly improved the therapeutic effect of chemotherapy or radiotherapy, without significant adverse reactions (78, 79). The mechanisms were speculated as: increased vascular permeability, interstitial microconvection and perfusion, then cause increased local drug levels and improved tissue oxygenation (80).

CONCLUSIONS

In this study, the constructed delivery system VD-TSL showed good physicochemical features such as uniform particle size, near zero zeta potential, really proud entrapment efficiency, obvious thermo-sensitive characteristics and excellent *in vitro* stability under −20°C within 6 months. More importantly, the vesicles exhibited strong tumor inhibitory activities when they were combined with HT, both *in vitro* and *in vivo*. Based on the bio-distribution of TSL, we've made full use of the synergistic effects of VCR and DOX in tumor suppression, and the restriction of their toxicity. The promising results warrant future studies which involve improve *in vivo* study including survival analysis and tissue distribution of VD-TSL, as well as develop more potential drug combination encapsulated in TSL to achieving much greater therapeutic effects.

ACKNOWLEDGMENTS AND DISCLOSURES

Authors acknowledge the financial support from Important National Science & Technology Specific Projects (Grant No.2012ZX09301003-001-009) and National Science Foundation of China (No. 81202466). We have no conflicts of interest to declare. And we sincerely thank the reviewers for the many useful suggestions offered to improve this article.

REFERENCES

1. Dexter DL, Kowalski HM, Blazar BA, Fligiel Z, Vogel R, Heppner GH. Heterogeneity of tumor cells from a single mouse mammary tumor. Cancer Res. 1978;38:3174–81.
2. Spremulli E, Dexter D. Human tumor cell heterogeneity and metastasis. J Clin Oncol. 1983;1:496–509.
3. Wick MR, Scheithauer BW, Weiland LH, Bernatz PE. Primary thymic carcinomas. Am J Surg Pathol. 1982;6:613–30.
4. Shimosato Y, Kameya T, Nagai K, Suemasu K. Squamous cell carcinoma of the thymus: an analysis of eight cases. Am J Surg Pathol. 1977;1:109–21.
5. Weide LG, Ulbright TM, LoehrerSr PJ, Williams SD. Thymic carcinoma: a distinct clinical entity responsive to chemotherapy. Cancer. 1993;71:1219–23.
6. Kwong B, Liu H, Irvine DJ. Induction of potent anti-tumorresponses while eliminating systemic side effects via liposome-anchored combinatorial immunotherapy. Biomaterials. 2011;32:5134–47.
7. Siddiqui A, Gupta V, Liu YY, Nazzal S. Doxorubicin and MBO-asGCSoligo nucleotide loaded lipid nanoparticles overcome multidrug resistance in adriamycin resistant ovarian cancer cells (NCI/ADR-RES). Int J Pharm. 2012;431:222–9.
8. Pauwels EK, Erba P, Mariani G, Gomes CM. Multidrug resistance in cancer: its mechanism and its modulation. Drug News Perspect. 2007;20:371–7.
9. Kaufman D, Chabner BA. Clinical strategies for cancer treatment. In: Chabner BA, Longo DL, editors. The role of drugs, cancer chemotherapy and biotherapy,2nd ed. Philadelphia, PA: Lippincott-Raven; 1996. p. 1.
10. Krishnan V, Rajasekaran AK. Clinical nanomedicine: a solution to the chemotherapy conundrum in pediatric leukemia therapy. Clin Pharmacol Ther. 2014;95:168–78.
11. Liang XJ, Chen C, Zhao Y, Wang PC. Circumventing tumor resistance to chemo-therapy by nanotechnology, Multi-Drug Resistance in Cancer. Humana Press. 2010. p. 467–488.
12. Morton SW, Lee MJ, Deng ZJ, Dreaden EC, Siouve E, Shopsowitz KE, *et al.* A nanoparticle-based combination chemotherapy delivery system for enhanced tumor killing by dynamic rewiring of signaling pathways. Sci Signal. 2014;7:44.
13. Weiss RB. The anthracyclines: will we ever find a better doxorubicin? Semin Oncol. 1992;19:670–86.
14. Takemura G, Fujiwara H. Doxorubicin-induced cardiomyopathy from the cardiotoxic mechanisms to management. Prog Cardiovasc Dis. 2007;49:330–52.
15. Oliveira PJ, Bjork JA, Santos MS, Leino RL, Froberg MK, Moreno AJ, *et al.* Carvedilol mediated antioxidant protection against doxorubicin induced cardiac mitochondrial toxicity. Toxicol Appl Pharmacol. 2004;200:159–68.
16. Della PT, Imondi AR, Bernardi C, Podestà A, Moneta D, Riflettuto M, *et al.* Cardioprotection by dexrazoxane in rats treated with doxorubicin and paclitaxel. Cancer Chemother Pharmacol. 1999;44:138–42.
17. Stearn WT. Marcel Dekker. In: Taylor WI, Farnsworth NR, editors. The Catharanthus Lkaloids. New York: Plenum; 1975. p. 9.
18. Zhang H, Wang ZY, Gong W, Li ZP, Mei XG, Lv WL. Development and characteristics of temperature-sensitive liposomes for vinorelbine bitartrate. Int J Pharm. 2011;414:56–62.
19. Malawista S, Bensch K, Sato H. Vinblastine and griseofulvin reversibly disrupt the living mitotic spindle. Science. 1968;160:770.
20. Kaplan LD, Deitcher SR, Silverman JA, Morgan G. Phase II study of vincristine sulfate liposome injection (Marqibo) and rituximab for patients with relapsed and refractory diffuse large B-cell lymphoma or Mantle cell lymphoma in need of palliative therapy. Cl Lymph MyelomLeuk. 2014;14(1):37–42.
21. Deitcher OR, Glaspy J, Gonzalez R, Sato T, Bedikian AY, Segarini K, *et al.* High-dose vincristine sulfate liposome injection (Marqibo) is not associated with clinically meaningful hematologic toxicity. Cl Lymph MyelomLeuk. 2014;14(3):197–202.
22. Chatterjee K, Zhang J, Honbo N, Simonis U, Shaw R, Karliner JS. Acute vincristine pretreatment protects adult mouse cardiac myocytes from oxidative stress. J Mol Cell Cardiol. 2007;43:327–36.

23. Vincristine and Doxorubicin. http://www.drugbank.ca/.
24. Yatvin MB, Weinstein JN, Dennis WH, Blumenthal R. Design of liposomes for enhanced local release of drugs by hyperthermia. Science. 1978;202:1290–3.
25. Weinstein JN, Magin RL, Yatvin MB, Zaharko DS. Liposomes and local hyperthermia: selective delivery of methotrexate to heated tumors. Science. 1979;204:188–91.
26. Yatvin WJ, Dennis WH, Blumenthal R. Design of liposomes for enhanced local release of drugs byhyperthermia. Science. 1978;202:1290–3.
27. Needham D, Anyarambhatla G, Kong G, Dewhirst MW. A new temperature-sensitive liposome for use with mild hyperthermia: characterization and testing in a human tumor xenograft model. Cancer Res. 2000;60:1197–201.
28. Lindner LH, Eichhorn ME, Eibl H, Teichert N, Schmitt-Sody M, Issels RD, *et al*. Novel temperature-sensitive liposomes with prolonged circulation time. Clin Cancer Res. 2004;10:2168–78.
29. Paulides MM, Bakker JF, Neufeld E, van der Zee J, Jansen PP, Levendag PC, *et al*. The HYPER collar: a novel applicator for hyperthermia in the head and neck. Int J Hyperth. 2007;23:567–76.
30. Smet MD, Heijman E, Langereis S, Hijnen NM, Grull H. Magnetic resonance imaging of high intensity focused ultrasound mediated drug delivery from temperature-sensitive liposomes: an in vivo proof-of-concept study. J Control Release. 2011;150:102–10.
31. Greish K. Enhanced permeability and retention of macromolecular drugs in solid tumors: a royal gate for targeted anticancer nanomedicines. J Drug Target. 2007;15:457–64.
32. Matsumura Y, Maeda H. A new concept for macromolecular therapeutics in cancer chemotherapy: mechanism of tumoritropic accumulation of proteins and the antitumor agent smancs. Cancer Res. 1986;46:6387–92.
33. Bae YH, Park K. Targeted drug delivery to tumors: myths, reality and possibility. J Control Release. 2011;153:198–205.
34. Mayer LD, Bally MB, Loughrey H, Masin D, Cullis PR. Liposomal vincristine preparations which exhibit decreased drug toxicity and increased activity against murine L1210 and P388 tumors. Cancer Res. 1990;50:575–9.
35. Kanter PM, Klaich GM, Bullard GA, King JM, Bally MB, Mayer LD. Liposome encapsulated vincristine: preclinical toxicologic and pharmacologic comparison with free vincristine and empty liposomes in mice, rats and dogs. Anti-Cancer Drugs. 1994;5:579–90.
36. Chen Q, Tong S, Dewhirst MW, Yuan F. Targeting tumor microvessels using doxorubicin encapsulated in a novel thermosensitive liposome. Mol Cancer Ther. 2004;3:1311–7.
37. Secord AA, Jones EL, Hahn CA, Petros WP, Yu D, Havrilesky LJ, *et al*. Phase I/II trial of intravenous Doxil (R) and whole abdomen hyperthermia in patients with refractory ovarian cancer. Int J Hyperth. 2005;21:333–47.
38. Yarmolenko PS, Zhao Y, Landon C, Spasojevic I, Yuan F, Needham D, *et al*. Comparative effects of thermosensitive doxorubicin-containing liposomes and hyperthermia in human and murine tumours. Int J Hyperth. 2010;26:485–98.
39. Ta T, Bartolak-Suki E, Park EJ, Karrobi K, McDannold NJ, Porter TM. Localized delivery of doxorubicin in vivo from polymer-modified thermosensitive liposomes with MR-guided focused ultrasound-mediated heating. J Control Release. 2014;194:71–81.
40. Embree L, Gelmon KA, Tolcher AW, Hudon NJ, Heggie JR, Dedhar C, *et al*. Validation of a high-performance liquid chromatographic assay method for quantification of total vincristine sulfate in human plasma following administration of vincristine sulfate liposome injection. J Pharm Biomed Anal. 1997;16:675–87.
41. Krawczyk PM, Eppink B, Essers J, Stap J, Rodermond H, Odijk H, *et al*. Mild hyperthermia inhibits homologous recombination, induces BRCA2 degradation, and sensitizes cancer cells to poly(ADP-ribose) polymerase-1 inhibition. Proc Natl AcadSci USA. 2011;108:9851–6.
42. Kong G, Anyarambhatla G, Petros WP, Braun RD, Colvin OM, Needham D, *et al*. Efficacy of liposomes and hyperthermia in a human tumor xenograft model: importance of triggered drug release. Cancer Res. 2000;60:6950–7.
43. Kong G, Braun RD, Dewhirst MW. Hyperthermia enables tumor-specific nanoparticle delivery: effect of particle size. Cancer Res. 2000;60:4440–5.
44. de Smet M, Langereis S, van den Bosch S, Grull H. Temperature-sensitive liposomes for doxorubicin delivery under MRI guidance. J Control Release. 2010;143:120–7.
45. Landon CD, Park JY, Needham D, Dewhirst MW. Nanoscale drug delivery and hyperthermia: the materials design and preclinical and clinical testing of Low temperature-sensitive liposomes used in combination with mild hyperthermia in the treatment of local cancer. Open Nanomed J. 2011;3:38–64.
46. Hossann M, Syunyaeva Z, Schmidt R, Zengerle A, Eibl H, Issels RD, *et al*. Proteins and cholesterol lipid vesicles are mediators of drug release from thermosensitive liposomes. J Control Release. 2012;162:400–6.
47. Hossann M, Wiggenhorn M, Schwerdt A, Wachholz K, Teichert N, Eibl H. In vitro stability and content release properties of phosphatidylglycero containing thermosensitive liposomes. Biochim Biophys Acta. 2007;1768:2491–9.
48. Yang Y, Yang YF, Xie XY, Wang ZY, Gong W, Zhang H, *et al*. Dual-modified liposomes with a two-photon-sensitive cell penetrating peptide and NGR ligand for siRNA targeting delivery. Biomaterials. 2015;48:84–96.
49. Johnston MJW, Semple SC, Klimuk SK, Edwards K, Eisenhardt ML, Leng EC, *et al*. Therapeutically optimized rates of drug release can be achieved by varying the drug-to-lipid ratio in liposomal vincristine formulations. Biochim Biophys Acta. 2006;1758:55–64.
50. Zhigaltseva IV, Maurer N, Akhong QF, Leone R, Leng E, Wang J, *et al*. Liposome-encapsulated vincristine, vinblastine and vinorelbine: A comparative study of drug loading and retention. J Control Release. 2005;104:103–11.
51. USP34-NF29.2011; 4585–887.
52. Dicheva BM, ten Hagen TLM, Schipper D, Seynhaeve ALB, van Rhoon GC, Eggermont AMM, *et al*. Targeted and heat-triggered doxorubicin delivery to tumors by dual targeted cationic thermosensitive liposomes. J Control Release. 2014;195:37–48.
53. Vehoveca T, Obreza A. Review of operating principle and applications of the charged aerosol detector. J Chromatogr A. 2010;1217:1549–56.
54. Joseph A, Rustum A. Development and validation of a RP-HPLC method for the determination of gentamicin sulfate and its related substances in a pharmaceutical cream using a short pentafluorophenyl column and a charged aerosol detector. J Pharm Biomed. 2010;51:521–31.
55. Yang YF, Yang Y, Xie XY, Cai XS, Zhang H, Gong W, *et al*. PEGylated liposomes with NGR ligand and heat-activable cell-penetrating peptide doxorubicin conjugate for tumor-specific therapy. Biomaterials. 2014;35:4368–81.
56. Ara MN, Matsuda T, Hyodo M, Sakurai Y, Hatakeyama H, Ohga N, *et al*. An aptamer ligand based liposomal nanocarrier system that targets tumor endothelial cells. Biomaterials. 2014;35:7110–20.
57. Li L, ten Hagen TLM, Hossann M, Süss R, van Rhoon GC, Eggermont AMM, *et al*. Mild hyperthermia triggered doxorubicin release from optimized stealth thermosensitive liposomes improves intratumoral drug delivery and efficacy. J Control Release. 2013;168:142–50.
58. Zhao Y, Alakhova DY, Kim JO, Bronich TK, Kabanov AV. A simple way to enhance Doxil® therapy: drug release from liposomes at the tumor site by amphiphilic block copolymer. J Control Release. 2013;168:61–9.

59. Al-Ahmady ZS, Chaloin O, Kostarelos K. Monoclonal antibody-targeted, temperature-sensitive liposomes: In vivo tumor chemotherapeutics in combination with mild hyperthermia. J Control Release. 2014;196:332–43.
60. Elias L, Portlock CS, Rosenberg SA. Combination chemotherapy of diffuse histiocytic lymphoma with cyclophosphamide, adriamycin, vincristine and prednisone (CHOP). Cancer. 1978;42:1705–10.
61. Arndt CAS, Nascimento AG, Schroeder G, Schomberg PJ, Neglia JP, Sencer SF, *et al*. Treatment of intermediate risk Rhabdomyosarcoma and undifferentiated sarcoma with alternating cycles of vincristine/ doxorubicin/ cyclophosphamide and etoposide/ ifosfamide. Eur J Cancer. 1998;34:1224–9.
62. Hofmeister CC, Jansak B, Denlinger N, Kraut EH, Benson DM, Farag SS. Phase II clinical trial of arsenic trioxide with liposomal doxorubicin, vincristine, and dexamethasone in newly diagnosed multiple myeloma. Leuk Res. 2008;32:1295–8.
63. Augustinus DGK, Henrie Ètte WAB, Dew D, Sonja HL, van der Holt B, van't Veer MB. Cyclophosphamide, doxorubicin, vincristine and prednisone chemotherapy and radiotherapy for stage I intermediate or high grade non-Hodgkin's lymphomas: results of a strategy that adapts radiotherapy dose to the response after chemotherapy. Radiother Oncol. 2001;58:251–5.
64. Kawasaki H, Taira N, Ichi T, Yohena T, Kawabata T, Ishikawa K. Weekly chemotherapy with cisplatin, vincristine, doxorubicin, and etoposide followed by surgery for thymic carcinoma. EJSO. 2014;40:1151–5.
65. Maruyama K. Intracellular targeting delivery of liposomal drugs to solid tumors based on EPR effects. Adv Drug Deliv Rev. 2011;63:161–9.
66. Allen TM, Hansen C, Martin F, Redemann C, Yau-Young A. Liposomes containing synthetic lipid derivatives of poly (ethylene glycol) show prolonged circulation half-lives in vivo. Biochim Biophys Acta. 1991;1066:29–36.
67. May JP, Li SD. Thermosensitive liposomes in cancer therapy. Recent Pat Biomed Eng. 2012;5:148–58.
68. Koning GA, Eggermont AM, Lindner LH, ten Hagen TL. Hyperthermia and thermo-sensitive liposomes for improved delivery of chemotherapeutic drugs to solid tumors. Pharm Res. 2010;27:1750–4.
69. Ta T, Porter TM. Thermosensitive liposomes for localized delivery and triggered release of chemotherapy. J Control Release. 2013;169:112–25.
70. Yatvin MB, Weinstein JN, Dennis WH, Blumenthal R. Design of liposomes for enhanced local release of drugs by hyperthermia. Science. 1978;202:1290–3.
71. Gaber MH, Hong K, Huang SK, Papahadjopoulos D. Thermosensitive sterically stabilized liposomes: formulation and in vitro studies on mechanism of doxorubicin release by bovine serum and human plasma. Pharm Res. 1995;12:1407–16.
72. Dordal MS, Winter JN, Atkinson AJJ. Kinetic analysis of P-glycoprotein-mediated doxorubicin efflux. J Pharmacol Exp Ther. 1992;263:762–6.
73. Celia C, Trapasso E, Cosco D, Paolino D, Fresta M. Turbiscan® Expertanalysis of the stability of ethosomes and ultra deformable liposomes containing a bilayer fluidizing agent. Colloids Surf B: Biointerfaces. 2009;72:155–60.
74. Yang ZB, Gong W, Wang ZY, Li BS, Li MY, Xie XY, *et al*. A novel drug-polyethylene glycol liquid compound method to prepare10-hydroxycamptothecin loaded human serum albumin nanoparticle. Int J Pharm. 2015;490:412–28.
75. Holzgrabe U, Nap CJ, Almeling S. Control of impurities in l-aspartic acid and l-alanine by high-performance liquid chromatography coupled with a corona charged aerosol detector. J Chromatogr A. 2010;1217(3):294–301.
76. Dunne M, Zheng J, Rosenblat J, Jaffray DA. Allen C.APN/CD 13-targeting as a strategy to alter the tumor accumulation of liposomes. J Control Release. 2011;154:298–305.
77. Viglianti BL. Target molecular therapies: methods to enhance and monitor tumor drug delivery. Abdom Imaging. 2009;34:686–95.
78. van der Zee J, Gonzalez GD, van Rhoon GC, van Dijk JD, van Putten WL, Hart AA. Comparison of radiotherapy alone with radiotherapy plus hyperthermia in locally advanced pelvic tumors: a prospective, randomised, multicentre trial. Dutch Deep Hyperth Group Lancet. 2000;355:1119–25.
79. Issels RD, Lindner LH, Verweij J, Wust P, Reichardt P, Schem BC, *et al*. Neo-adjuvant chemotherapy alone or with regional hyperthermia for localised high-risk soft-tissue sarcoma: a randomised phase 3 multicentre study. Lancet Oncol. 2010;11:561–70.
80. Song CW. Effect of local hyperthermia on blood flow and microenvironment: a review. Cancer Res. 1984;44:4721s–30s.